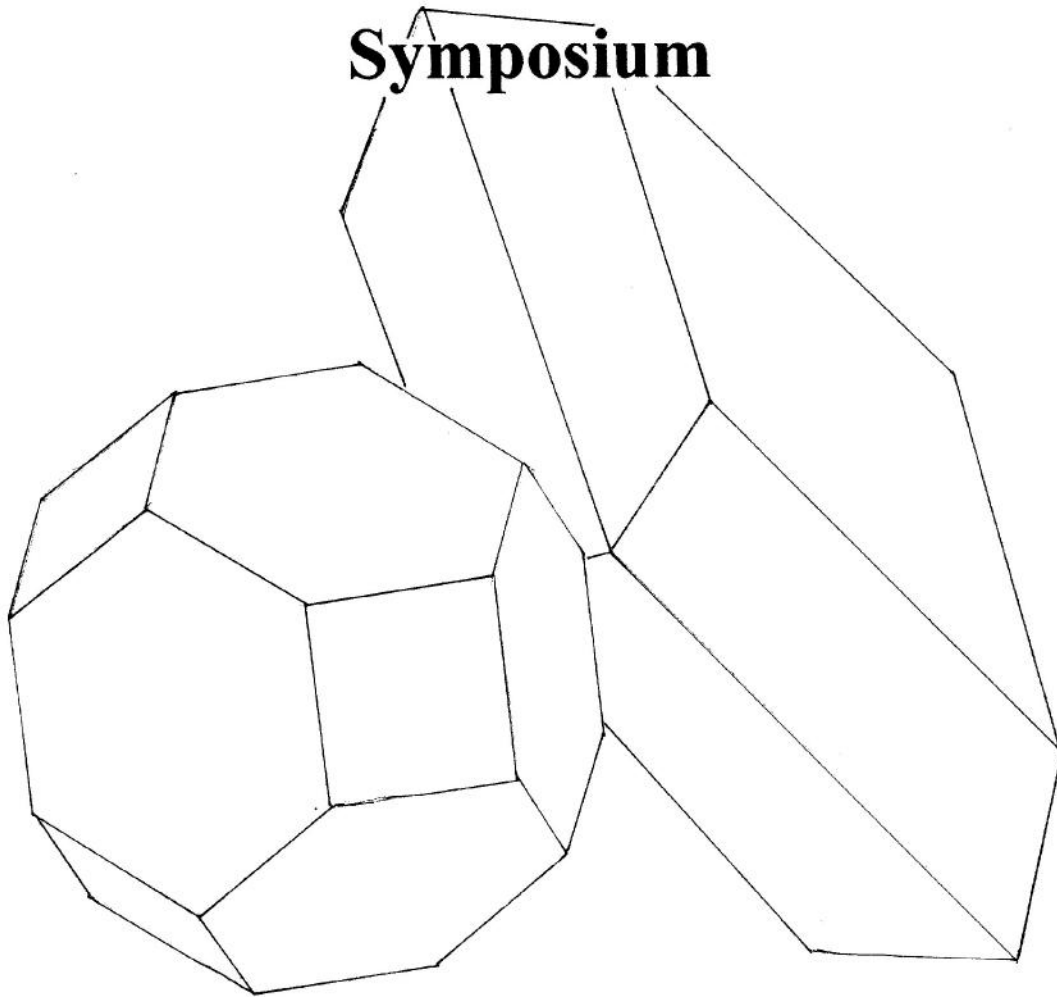# The 47th

Rochester Mineralogical Symposium

April 25, 2020

S. ROBINSON

47th Rochester Mineralogical Symposium
The eRMS, April 25, 2020

Chair – Raymond McDougall

Registrar – Carl Miller

Online Coordinator and Host – John Rakovan

Treasurer – Dan Imel

Technical Session – Sarah Hanson

Past Chair and Senior Advisor – Steve Chamberlain

What's New in Minerals – Jeff Scovil, John Betts

Program Notes – Raymond McDougall, Sarah Hanson

Program Notes Cover Art – Susan Robinson

Technical and Website Support – Paul Dudley, Dan Imel

Symposium Committee – John Betts, Steve Chamberlain, Betty Fetter, Bruce Gaber, Sarah Hanson, Dan Imel, Brian McGrath, Raymond McDougall, Carl Miller, Bob Morgan, John Rakovan

And thanks to all who were ready in all of their Symposium respective roles, had we managed to gather in person:

Bruce Gaber, Carl Francis, Brian McGrath, Quintin Wight, Gloria Staebler, Michael Bainbridge, Tom White, Dan Sperber, Lauren Imel, Laurie Steele Sperber, Charlene Freundlich
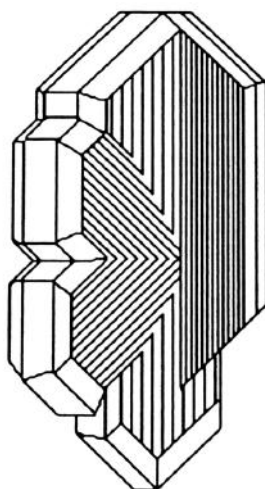
TABLE OF CONTENTS

Welcome to the eRMS 2020!

Welcome to the 47th Rochester Mineralogical Symposium: the eRMS 2020.

Of course it is not as we had originally planned, due to the global coronavirus pandemic. We were disappointed that we had to cancel. However, we are thrilled that the spirit of the Rochester Symposium prevailed, such that we could gather online for an afternoon of presentations.

We had planned a great lineup of featured 2020 speakers and we are delighted that almost all have already confirmed that they will speak when we are all next together in Rochester. So the featured talks will go on at the next RMS!

The eRMS focused on the two areas of what we do each year at the Symposium that are time sensitive: (1) What's New in Minerals and (2) new research and technical presentations. These two areas are at the core of the RMS.

If you missed the eRMS for any reason, the presentations set out in the Program are all included on the Rochester Mineralogical Symposium channel on YouTube, in a playlist at this link:

> https://bit.ly/eRMS2020

For all of you who participated, we're so grateful for your continuing support. The Symposium is a springtime reunion of mineral friends – we look forward to it each year and it would absolutely not be the same without you. And if a global pandemic means we have to be together online, then so be it. It was great to see Rochester's unsinkable spirit at the eRMS, complete with humour, laughs, a raised glass and mineral songs.

We'll see what the future has in store for us all over the next year, but we are sure planning to hold the Rochester Mineralogical Symposium at the Radisson Rochester Airport Hotel, April 15-18, 2021. Write it into your calendar!

We will communicate by email about future developments, so if you think we might not have your current email address, please let us know at contactrms@hotmail.com. You can also follow the Rochester Mineralogical Symposium on Facebook.

Stay well!
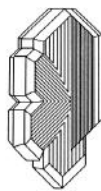
47th ROCHESTER MINERALOGICAL SYMPOSIUM: THE eRMS 2020!

PROGRAM

Saturday, April 25, 2020

12:00 pm	Join Online Meeting
12:05 pm	**Opening - *Raymond McDougall***
12:15 pm	**What's New In Minerals - *Jeff Scovil***
1:00 pm	**Mystery Subject! – *John Jaszczak***
1:05 pm	**What's New in Minerals II – *John Betts, with Raymond McDougall and Mark Jacobson***
2:45 pm	**Fibrous zinc sulfide from the Francon Quarry, Montreal, Canada. *J. Fink**, *C. Emproto, and J. Chappell*
3:00 pm	**Halogen and trace-element chemistry of crustal carbonatite-hosted apatite in the Grenville Province**. *C. Emproto*, *S. Mounce, J. Fink, and J. Rakovan*
3:15 pm	**Melt and micromineral inclusions in fluorapatite, calcite, fluorite, albite, and augite from the Schickler occurrence, ON, Canada. *S. Mounce**, *C. Emproto, M. Murchland, M. Rutherford, and J. Rakovan*
3:30 pm	**Optically anomalous crystals**. *M. Rutherford**, *M. Murchland, J. Fink, and J. Rakovan*
3:45 pm	**Optical anomalies in flattened inclusions from muscovite**. *M. Murchland*, *M. Rutherford, J. Fink, and J. Rakovan*
4:00 pm	**Neutron diffraction and resonance absorption spectroscopy study of the Harvard wire gold, Groundhog Mine, Colorado**. *J. Rakovan**, *R. Alonso-Perez, F. Keutsch, S. Vogel, A.S. Losko and A. Long.*
4:15 pm	**Silver content of wire gold; implications for growth mechanism**. *C. J. Anderson** *and J. Rakovan*
4:30 pm	**<u>GRAND FINALE</u> – *David K. Joyce* – Raise a Glass and Sing!**

Raymond McDougall - Chairman <mcdougallray@gmail.com >
Carl Miller - Registrar (804) 517-6709 <contactrms@hotmail.com>
John Rakovan – Online Host for the eRMS 2020
Sarah Hanson – Technical Session Coordinator <slhanson@adrian.edu>

THE THIRTY-SEVENTH TECHNICAL SESSION of the Rochester Mineralogical Symposium was held, in part, online. Abstracts were reviewed by a committee consisting of Dr. Steve Chamberlain, New York State Museum; Alexander Falster and Dr. Carl Francis, Maine Mineral and Gem Museum; Dr. Sarah Hanson, Adrian College; Dr. Marian Lupulescu, New York State Museum; and Dr. George Robinson, St. Lawrence University. We would like to issue a warm welcome to the newest member of the Abstract Review Panel, Alexander Falster. Welcome aboard!

Seven of the abstracts were presented at the e-meeting and seven were accepted for publication only. Four were carried over until next year and will be presented and published during the symposium in 2021. Abstracts that were presented at the 2020 eRMS are denoted with an asterisk.

*SILVER CONTENT OF WIRE GOLD; IMPLICATIONS FOR GROWTH MECHANISM. <u>*C. J. Anderson*</u> *and J. Rakovan*, Dept. of Geology and Environmental Earth Science, 250 S. Patterson Ave., Miami University, Oxford, OH, 45056.

Wire gold is an exceptionally rare habit of native gold, known from only a handful of deposits worldwide (Anderson and Rakovan 2017). In contrast to gold "pseudo wires" or "ribbons," which are actually elongate spinel twins (Mauthner 2004), wire gold is characterized by the same longitudinal striations and lock-of-hair morphology as wire silver.

Our recent work indicates that wire silver's unique texture and morphology are generated by solid-state ion conduction of Ag^+ ions through a laterally constrained phase transformation in Ag_2S (Anderson et al. 2019).

Given the strong similarities in appearance between wire gold and silver, we hypothesize that wire gold may form by the same or similar processes. Furthermore, the vast majority of naturally-occurring ion-conductors contain structural Ag. Thus, we predict that all wire gold will contain a significant amount of Ag.

Rakovan et al. (2020) analyzed the surface and bulk chemistry of two wire gold specimens and found significant concentrations of Ag. We have analyzed the surface elemental composition of 4 additional wire gold specimens by energy dispersive spectroscopy (EDS); one specimen is a cm-long wire on matrix from Ground Hog Mine, Eagle County, Colorado, and the other three are from placers in Bolívar, Venezuela, ranging from 0.5 to 1 cm long. EDS revealed that the minimum Ag content in our samples is 37±6 at% (25±6 wt%), and as much as 72±6 at% Ag (Table 1). No other elements besides Au and Ag were detected (instrument detection limit is about 0.5 wt%).

The GHM-1 sample is unique among those analyzed in that the wire is attached to a matrix on which it grew (Figure 1). The matrix material of GHM-1, besides Au and Ag, notably contained Te, with a 3-measurement average (likely consisting of multiple phases) of 37±5 wt% Te. The average Au/Ag atom ratio of the matrix (≈1:5) is somewhere between that of Petzite (≈1:3) and Hessite (0:1), both of which are known from the Ground Hog Mine (Lovering et al. 1978).

Based on the high Ag content of these wire gold specimens, as well as the association with Ag/Au tellurides in the Ground Hog Mine, we suggest that wire gold may form by solid-state ion-conduction of Au^+ through a Ag/Au telluride phase, analogous to wire silver growth from Ag sulfide.

Table 1. EDS analysis of Ag content in gold wires.		
Sample	Locality	Ag at%
GHM-1	Ground Hog Mine, CO	38 ± 6
VEN-1	Bolívar, Venezuela	72 ± 6
VEN-2	Bolívar, Venezuela	37 ± 6
VEN-3	Bolívar, Venezuela	38 ± 5

*Values are averages of three measurements, taken near the bottom, middle & top of each specimen.

Figure 1. Specimen GHM-1. Wire gold on matrix from Ground Hog Mine, Eagle County, Colorado. Approximately 2 cm tall. Collector's Edge specimen.

REFERENCES

Anderson, C.J., J. Rakovan, R. Mathur, and A, Tremsin. 2019. Natural solid-state ion conduction induces metal isotope fractionation. *Geology*, 47:617-621.

Anderson, C.J., and J. Rakovan. 2017. Connoisseur's Choice: Wire Silver, Kongsberg, Norway & Wire Gold, Ground Hog Mine, Gilman, Colorado. *Rocks & Minerals*, 92:344-357.

Lovering, T., O. Tweto, and T. Lovering. 1978. Ore deposits of the Gilman district, Eagle County, Colorado; Geological Survery Professional Paper 1017. Washington D.C.: U.S. Government Printing Office, p.54,69.

Mauthner, M. 2004. Morphology of gold crystals from the Yukon Territory, Canada. *Rocks & Minerals*, 79:100-109.

Rakovan, J., R. Alonso-Perez, F. Keutsch, S. Vogel, A. Losko, and A. Long. 2020. Neutron diffraction and resonance absorption spectroscopy study of the Harvard wire gold, Ground Hog Mine, Colorado. *Forty-seventh Rochester Mineralogical Symposium: Contributed Papers in Specimen Mineralogy,* Program with abstracts.

NEW DATA ON THE BEILKE, SCHUETTE, AND WIMMER GRUS QUARRIES, MARATHON COUNTY, WISCONSIN. *T.W. Buchholz[1], A.U. Falster[2] and W.B. Simmons[2]* [1]1140 12th Street North, Wisconsin Rapids, Wisconsin 54494, [2]MP[2] Research Group, Maine Mineral & Gem Museum, PO Box 500, 99 Main Street, Bethel, Maine 04217, USA.

Recently micro and thumbnail samples from the late Walter Taminnen collection became available, opening a window into materials collected from the Beilke, Schuette, and Wimmer Grus quarries from the 1970s to the early 1990s. Located in the NE portion of the Proterozoic Nine Mile granite (1505.9 ± 2.7 Ma, Dewane & Van Schmus, 2007), Marathon County, Wisconsin, these sites were all closed and reclaimed by 1998. The Taminnen samples, in part prepared as heavy mineral separates, provide an opportunity to evaluate the mineralogy of material from locations no longer accessible and in light of advances in instrumentation, methodologies and mineral redefinitions.

Monazite group species: This material was previously identified as cheralite, but this mineral species has been redefined (Linthout, 2007), thus this material is a monazite group mineral. It has variable REE/(Ca+Th) up to 0.40 and REE/TH of 0.25, which places this material in the monazite field. Both high and low Th monazites are present. Additionally, there are La, Ce, and Nd-dominant monazite species.

Bastnäsite group species: In the 1970s to early 1990s, bastnäsite group species were much less complicated. We have now identified, from samples of what was then called just 'bastnäsite', La-, Ce-, Nd-dominant members which occur both as F- and OH-dominant species to yield six species total. In addition, synchysite-parisite species occur also. The high Ca content is the distinction between the species: no Ca in bastnäsite, Ca:REE =1:1 in synchysite and Ca:REE = 1:2 in parisite.

Cerianite-(Ce): Small grains of cerianite-(Ce) are common in the heavy mineral separates, and one grain of monazite (or rhabdophane) shows similar Ce-dominance.

Ferrimolybdite: In the examination of samples of rutile, a number of samples were noted with small pale yellow bladed crystals. In polished section, the pale-yellow mineral was determined to be ferrimolybdite. Virtually all samples are associated with rutile, and perhaps some brookite. Additionally, numerous tiny yellow flakes of ferrimolybdite were recovered in heavy mineral separates. In the 1980s, molybdenite was frequently found at these locations, though none was found in this study.

Ti oxide species: In the past, Ti oxide species (anatase, brookite, rutile, with anatase being most common) were very common in the northern segment of the Nine Mile pluton. Some of these have retained the original structures but many have undergone partial or complete paramorphism, e.g., from brookite or anatase to rutile. The more recently worked areas to the SW and S of the pluton only rarely produce these minerals. In the examination of the ferrimolybdite material, the polished section included an exposure of rutile. Distinct patchy zonation was observed. Brighter portions are distinctly enriched in Nb and Ta.

Ixiolite-like unknown material: Small grains of a Nb-dominant, U-rich mineral, possibly related to ixiolite, are common in one heavy mineral separate. The composition does not match any known ixiolite-like phase.

Tourmaline: One sample of a red-brown tourmaline group mineral on matrix was included in the collection and appears to fall along the schorl-elbaite series. Although tourmaline-group minerals are extremely scarce in the complex, the matrix of this sample is identical to the other samples and the tourmaline is consistent with the very few other samples known.

REFERENCES

Dewane, T. J. and W. R. Van Schmus. 2007. U-Pb geochronology of the Wolf River batholith, north-central Wisconsin: Evidence for successive magmatism between 1484 Ma and 1468 Ma. *Precambrian Research*, 157:215-234.

Falster, A.U., T.W. Buchholz and Wm. B. Simmons. 2012. Mineralogical and mineral-chemical heterogeneity indicated by the distribution of accessory minerals in pegmatites of the Nine Mile pluton of the Wausau syenite complex, Marathon Co., Wisconsin. *Canadian Mineralogist,* 50:1055-1070.

Linthout, K. 2007. Tripartite division of the system 2REEPO4 – CaTh(PO$_4$)$_2$– 2ThSiO$_4$, discreditation of brabantite, and recognition of cheralite as the name for members dominated by CaTh(PO4)$_2$. *Canadian Mineralogist*. 45:503-508.

*HALOGEN AND TRACE ELEMENT CHEMISTRY OF CRUSTAL CARBONATITE-HOSTED APATITE IN THE GRENVILLE PROVINCE. *C. Emproto, J. Fink, S. Mounce, and J. Rakovan*, Miami University, Department of Geology and Environmental Earth Science, Oxford, Ohio, 45056.

Grenville-aged rocks exposed in Ontario, Quebec, and New York are a geological treasure trove for geoscientists and mineral collectors alike. Some of the most spectacular mineral deposits in this region occur as narrow bodies of calcite ± apatite, etc. with coarsely crystallized silicate margins of a mineralogy variably reflective of that of the host rock. These deposits are colloquially known as "vein dikes" and are renowned for producing exceptionally large and well-formed crystals of many rock-forming minerals. Despite a long and storied history of resource exploration and exploitation for mica, phosphate, and mineral specimens, vein dikes have presented petrological questions to geologists since the mid-19th century. Recent isotopic and textural studies suggest that vein dikes form from the partial melting and mobilization of crustal carbonate rocks during the collapse of orogenic belts, and are thus crustally-derived carbonatites. Although answers as to the origin of crustal carbonatites appear to have been broadly answered, many questions remain regarding their emplacement. The coarse and heterogeneous crystallization of crustal carbonatites renders assessment of their bulk chemistry difficult. Apatite group minerals are nearly ubiquitous in crustal carbonatites. This, combined with their ability to structurally accommodate a diverse array of elements including rare earth elements and halogens makes apatite group minerals a promising source of information for systematically assessing the chemistry of crustal carbonatites. Apatite samples from ~40 discrete localities were analyzed using single crystal X-ray diffraction (SCXRD) to determine the halogen composition and laser ablation inductively coupled plasma mass spectrometry (LA-ICP-MS) to assess the trace element composition. Localities were grouped by geographic distribution

and general mineralogy. From the distribution of known deposits, several clusters of swarms are apparent. The Bear Lake, Wilberforce, Bancroft, Lake Clear, Yates, and Aumond localities and nearby occurrences comprise a trend in the northwestern portion of the study area, whereas localities near and between Verona, ON and Wakefield, QC along with the Kelly Farm in New York comprise a trend in the southeastern portion of the study area. Apatite chemistry was further used to subdivide these groups. SCXRD structure solutions with refined site occupancies suggest that the vast majority of apatite from crustal carbonatites is hydroxyl-rich fluorapatite of the approximate composition F:OH ~60:40. Hydroxylapatite, chlorapatite and rare sub-ternary compositions also occur. Apatite with detectable Cl is nearly absent from the northwestern trend of crustal carbonatites, yet is very common in the southeastern group. This may suggest that the metasomatic fluids melting the source rocks of many of the carbonatites in the southeastern trend were Cl-bearing, or that the source rocks themselves contained significant Cl. Chondrite-normalized plots of rare earth element (REE) concentrations show slight Eu anomalies with light rare earth element (LREE) enrichment. Trace element data indicates that Si substitution is the dominant coupled substitution for trivalent REE incorporation in crustal carbonatite apatite, but that Na coupled substitution is also of variable importance. Some localities, such as the Yates Mine, have negligible Na coupled substitution as a mechanism for REE incorporation.

Figure 1. Google Earth image of the study area with sampled crustal carbonatite localities marked with gray circles. The northwestern (NW) and southeastern (SE) groups are separated with a black line.
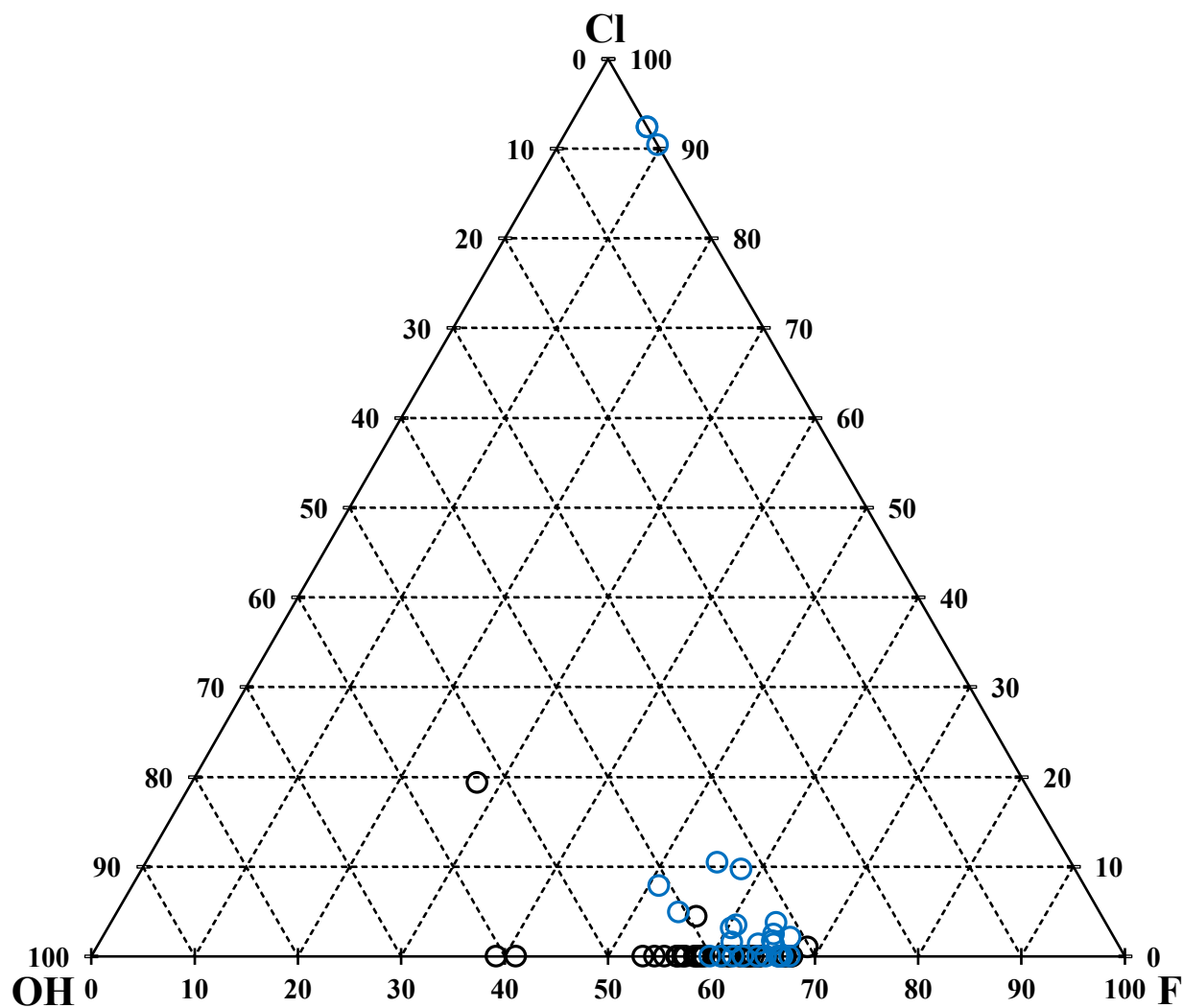
Figure 2. Ternary plot of apatite halogen compositions modeled from SCXRD crystal structure refinements (N=59). Black circles represent data from apatite from the NW group whereas blue circles represent the SE group.

JUXTAPOSED OXIDIZNG AND REDUCING LATE-STAGE ENVIRONMENTS IN THE EMMONS PEGMATITE, UNCLE TOM MOUNTAIN, GREENWOOD, OXFORD COUNTY, MAINE. _A.U. Falster_ and _W.B. Simmons_, Maine Gem and Mineral Museum, PO Box 500, 99 Main St, Bethel, ME, 04217.

Recent finds at the Emmons pegmatite on Uncle Tom Mountain, Greenwood, Oxford Co., Maine have revealed a secondary phosphate assemblage formed from low-temperature alteration of the primary lithiophilite masses. Recent work has identified six masses of lithiophilite ranging from 15 to 80 cm in maximum dimension. The juxtaposed oxidized and reduced assemblages occur where two 1.5 m masses had merged. The lithiophilite masses are typically intimately associated with montebrasite masses up to 45 cm in maximum dimension. The primary lithiophilite masses occur in the core zone which is outlined by a 3-12 cm thick ball muscovite band with the convex surfaces of the rounded muscovite masses pointing toward the core. The ball muscovite on the concave side away from the core is associated with book muscovite.

The montebrasite appears to be affected by manganese-rich hydrothermal fluids, similar to those Berman and Gonyer (1930) described at the Berry Havey pegmatite in Poland, Androscoggin Co., Maine.

High activity of carbonate ions led to abundant and porous or vuggy rhodochrosite. In these cavities, a secondary phosphate association consisting of eosphorite-childrenite + reddingite + dickinsonite + fairfieldite + "apatite" formed. The last alteration process transformed reddingite, $(Mn^{2+},Fe^{2+})_3(PO_4)_2 \cdot 3H_2O$, to landesite $Mn^{2+}_{3-x}Fe^{3+}_x(PO_4)_2(OH)_x$ $(3-x)H_2O$ (Berman and Gonyer 1930). Recently, the rare mineral correianevesite, $Fe^{2+}Mn^{2+}_2(PO_4)_2$ $3H_2O$ has been found as part of an assemblage formed under non-oxidizing conditions (pers. comm. Pietro Vignola). This is the third world occurrence of this mineral.

The association commonly consists also of abundant late fluorapatite that ranges in color from yellow to near colorless and, in one case, almost colorless sphalerite. Evidently, all Fe is being partitioned into the phosphates.

The presence of sphalerite among the secondary phosphates attest to non-oxidizing conditions. However, very close-by, within a few centimeters, clearly oxidizing conditions produced an assemblage of strunzite, jahnsite group species, kryzhanovskite, laueite, pseudolaueite, stewartite, beraunite, mitridatite, bermanite and similar species. These species are forming under a comparable temperature (Simmons et al. 2003). This suggests that there exist micro-environments with distinctly different conditions regarding Eh, pH, and ions present. These small-scale environments do not communicate with each other and follow their own distinctive path of evolution.

REFERENCES

Berman, H. and F.A. Gonyer. 1930. Pegmatite minerals of Poland, Maine. _American Mineralogist_ 15:375-387.
Simmons, W. B., K.L. Webber, A.U. Falster, and J.W. Nizamoff. 2003. Pegmatology Pegmatite Mineralogy Petrology and Petrogenesis. Rubellite Press, 176 p.

*FIBROUS ZINC SULFIDE FROM THE FRANCON QUARRY, MONTREAL, CANADA. *J. Fink[1], C. Emproto[1], and J. Chappell[2]*, [1]Department of Geology and Environmental Earth Science, Miami University, Oxford, Ohio, 45056, [2]Department of Geology and Geological Engineering, Colorado School of Mines, Golden, Colorado, 80401.

The Francon quarry in Montreal hosts several silicocarbonatite sills renowned by mineralogists and collectors alike for their unusual mineralogy and world class mineral specimens. These sills are part of the Monteregian Hills, which include Mont Royal and Mont St. Hilaire. Prior to this study, zinc sulfide was known to occur at Francon quarry as either wurtzite or sphalerite, the latter being more common. Both minerals exhibit closest packing of S ions and their structures differ in the stacking arrangement of individual layers. Wurtzite is only known at Francon quarry from a single crystal on one sample. This crystal exhibited hemimorphic morphology commonly seen in wurtzite. Sphalerite is more commonly found at Francon and exhibits more complex morphologies than that of wurtzite. Zinc sulfide of an unusual fibrous habit has been identified in recently processed rough material collected prior to the quarry's closure in 1981. In this material, ZnS occurs as conical bundles of elongated tan crystals with a silky luster (Figure 1). These crystals are associated with weloganite, calcite, quartz, franconite, baryte, and an unknown mineral [UM1990-28-OHF:Al]. Scanning electron microscopy X-ray energy dispersive spectroscopy (SEM-XEDS) analyses confirm a chemistry of Zn and S. Unusual for wurtzite and sphalerite is the absence of Fe above the ~1 wt% detection limit of our instrument, suggesting that this material is essentially Fe-free. Raman spectroscopy was inconclusive due to the similarities in indexed sphalerite and wurtzite patterns. Polarized light microscopy precludes sphalerite as the sole phase due to birefringence and coherent parallel extinction exhibited in the fibers. Electron back-scattered diffraction (EBSD) produced kikuchi bands indexable by the wurtzite structure. Single crystal X-ray diffraction data suggests a hexagonal unit cell with cell parameters ($a=3.80$Å, $b=3.84$Å, $c=9.36$Å, $\alpha=89.76°$, $\beta=90.00°$, $\gamma=60.10°$), inconsistent with the most common wurtzite polytype, wurtzite-2H. The *c* dimension indicates a 3-layer polytype, which is not known for wurtzite. Closest packing with a 3-layer repeat (ABC stacking) yields cubic symmetry and the structure of sphalerite, inconsistent with the observed optical properties. The identity of these crystals is still unknown due to discrepancies in structure modelling from single crystal X-ray diffraction data, although most data suggest wurtzite.
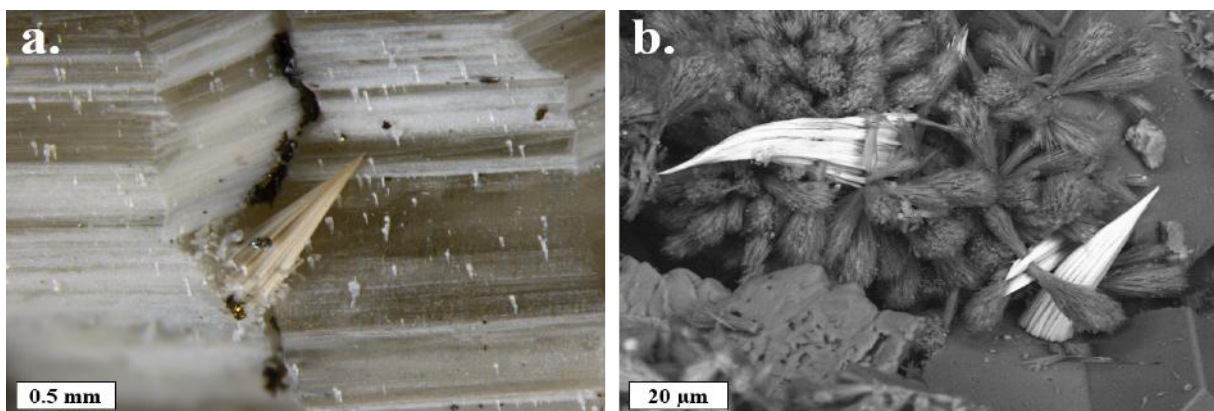

Figure 1. Bundles of fibrous ZnS imaged using (a.) light microscopy and (b.) SEM backscattered electron imaging (BSEI) (b.). In the BSEI image, ZnS (bright) occurs associated with UM1990-28-OHF:Al (darker acicular bundles).
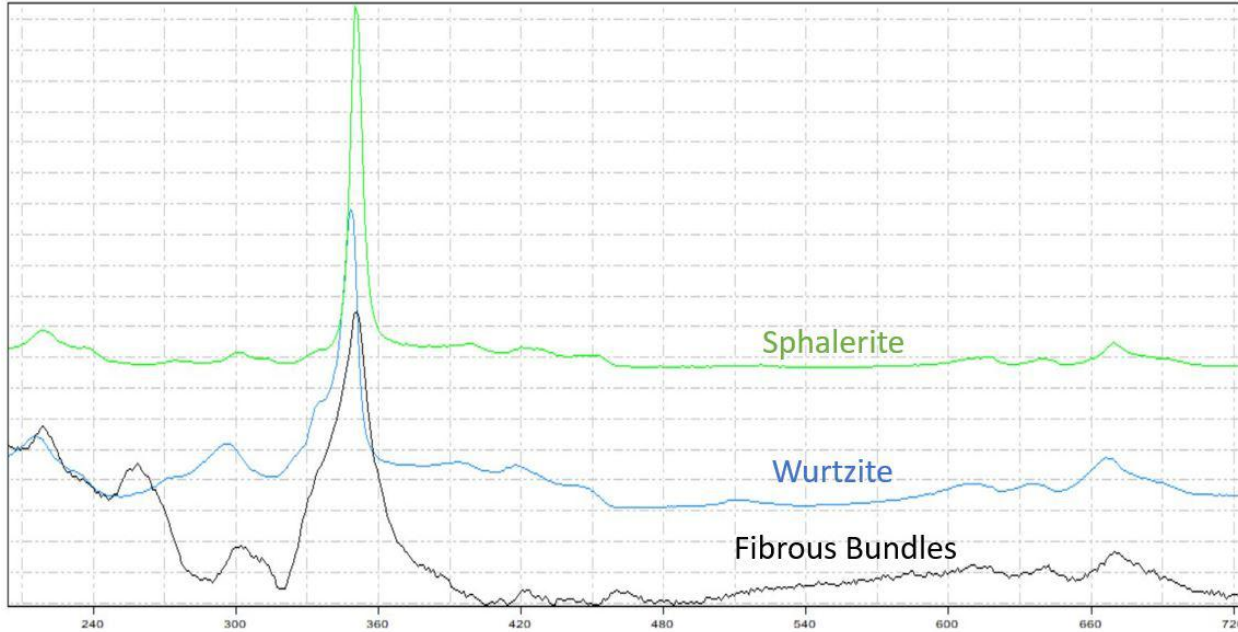
Figure 2. Raman spectroscopy scan of fibrous ZnS crystals. Raman spectroscopy confirms the identity of these bundles to be either wurtzite or sphalerite. However, this method cannot distinguish between the two phases.

AN UNUSUAL URANINITE REPLACEMENT MASS FROM THE HAYES PEGMATITE, NOYES MOUNTAIN, GREENWOOD, OXFORD CO., MAINE.

S.L. Hanson[1], A.U. Falster[2], and Wm. B. Simmons[2] Geology Dept. [1]Geology Department, Adrian College, 110 S. Madison St., Adrian, MI 49221, [2]MP[2] Research group, Maine Mineral & Gem Museum, 99 Main Street, Bethel, Maine 04217.

The Hayes pegmatite (aka Hayes Ledge Quarry), located on Noyes Mountain near Greenwood, Oxford county, Maine is a moderately evolved orogenic pegmatite in the Oxford Pegmatite Field. During the summer in 2017, Frank Perham and his mining crew opened a giant miarolitic cavity that reached a maximum dimension of about 80 m. Frank named the pocket the "Mother Mary Pocket" in honor of his wife. The pocket is most well-known for the several tons of spectacular quartz crystals that were recovered. The quartz occurred as single crystals, scepters, floaters, and large matrix specimens. The largest crystals reached up to 60 cm. Minor, heavily corroded, feldspar and accessory fluorapatite, beryl and pyrite replaced by goethite were also present. During the final stages of mining out the cavity, a small mass of yellow altered uraninite [UO_2] was recovered (Figure 1). The mass reached a maximum dimension of 2 cm and appears as a composite of smaller grains. In cross-section, the mass exhibits a few small areas where remaining uraninite was rimmed by orange to orange-yellow schoepite group species and possibly other uranyl oxy-hydroxide species. Interstitial brown-to-tan U-rich zircon is also present (Figure 2). The outer portion of the mass exhibits greater alteration as the secondary rimming schoepite group minerals are further altered to canary-yellow soddyite [$(UO_2)_2SiO_4 \cdot 2H_2O$]. In general, the replacement of schoepite group minerals by soddyite is only partial as some remnant of schoepite group species are present (Figure 2). Both the altered and unaltered

material is very low in Th and only has low levels of Pb which is not surprising since the age of the pegmatite is on the order of 250 Ma.

The presence of the canary yellow soddyite is surprising. This is because similar uraninite masses with secondary uranium species are well known from the Ruggles and Palermo pegmatites in New Hampshire. Schoepite, fourmarierite and related species are the secondary species in those locations. Soddyite has not been noted. Two years ago, a heavily uranium-mineralized garnet layer was exposed between the Hayes and Outback pegmatites in close proximity. There soddyite was also found but only in fracture fillings and not as distinct uraninite crystal replacements.

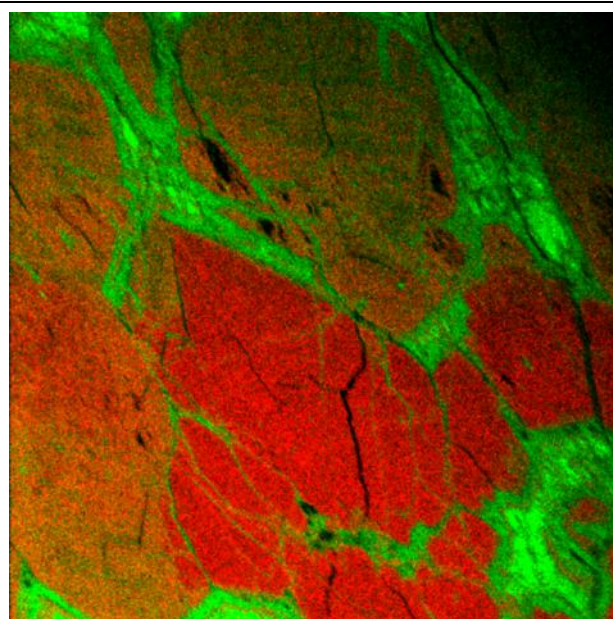|	
Figure 1. Photo of the uranium mineral-bearing pod from the Mother Mary pocket. Field of view is 2 cm.	**Figure 2.** SEM X-ray map across altered uraninite grains from the U-mineral-bearing mass. Schoepite group minerals exhibit bright red, soddeite grains (with greater Si) exhibit a more orange, mixed with green color on the map.

POLLUCITE FROM THE SINCLAIR CAESIUM MINE, WESTERN AUSTRALIA, AUSTRALIA; THE HIMALAYA MINE, CALIFORNIA, USA; THE ROSE QUARTZ CRYSTAL LOCALITY, NEWRY, MAINE, USA; AND THE VALOR LITHIUM AND CAESIUM PROSPECT, QUEBEC, CANADA. *Mark Ivan Jacobson*, 1714 S. Clarkson St., Denver, CO, 80210.

The occurrence of pollucite, $[(Cs,Na)_2Al_2Si_4O_{12} \cdot nH_2O]$, in pegmatites has been interpreted as evidence of extreme fractionation in a LCT pegmatite. It is also the primary ore for cesium, with only a limited number of known pegmatite localities worldwide and even fewer historic economic deposits. The specimens described here were all anhedral, typical of mined economic material.

The Sinclair Dome pegmatite trend is located within a north-south greenstone belt, northwest of Norseman, Western Australia, Australia. In October 2016, Pioneer Resources Ltd. of Perth, Western Australia announced the discovery of pollucite during reverse circulation drilling for spodumene. This pegmatite has a surface strike length of 800 meters and a true width of 150 meters. Evaluation of the pegmatite confirmed that pollucite was present in economic quantities, from what became the Sinclair Caesium mine. The pollucite zone does not outcrop, but lies beneath an outcropping microcline-rich zone. Other minerals intimately bordering the pollucite are petalite with eucryptite alteration, fine to medium grained lepidolite masses, quartz, and accessory minerals of amblygonite and zinnwaldite.

Pollucite has been known from the Himalaya mine, Mesa Grande, San Diego County, California since 1921 when Fred Rynerson encountered white masses underground that went to the dump during his mining for gem tourmalines. He reported that he had mined an estimated ten tons. Another large pod of pollucite was encountered during underground mining by Pala International in 1997, but was not publicized widely. Since its economic value was low, the material was left in place except for a small amount of material that was distributed locally. This later find of pollucite occupies the entire central area of the pegmatite where tourmaline gem pockets usually occur.

Pollucite from the Rose Quartz locality, Spur pegmatite of the Plumbago Mountain pegmatite, Newry, Oxford County, Maine was discovered in 2016 by Mike O'Neill, who was mining for rose quartz crystals and other vug minerals, and identified by Alexander Falster. The pollucite bearing zone is located about 1 meter below the hanging wall contact. Laterally the pollucite zone was exposed for 6 meters and was between 0.50 to 1 meter thick. The cleavelandite zone below the pollucite contained the desired rose quartz vugs with the occasional montebrasite, needle-like elbaite, columbite and other minerals. The footwall zone was composed of sugary to granular albite with rare tiny vugs.

Pollucite was identified on the outcrop of the southernmost Valor lithium and caesium pegmatite prospect, during its initial exploration in 1955. Except for three sample pits, the pegmatite has not been mined. During a visit to the pegmatite in July 2019, two glaciated outcrops of pollucite were located and exploited for specimens with hand tools. No cavities were seen. The pollucite was in association with cleavelandite, spodumene and rare fine-grained masses of lepidolite.

Pollucite samples from these localities were analyzed by SGS Canada, Inc. to confirm and document this mineral for comparison with other known pollucite localities. At least 50 grams per sample was provided for analysis. The seven major elements (Si, Al, Na, K, Fe, Mg, and P) plus LOI (interpreted to represent water) were determined by borate fusion and then x-ray fluorescence analysis. Lithium was determined by sodium peroxide fusion and then used Inductively Coupled Plasma - Atomic Emission Spectroscopy (ICP-AES). Rubidium was determined by crushing and compressing the sample into a pellet and then analyzed by x-ray fluorescence. Cesium was determined by sodium peroxide fusion and then Inductively Coupled Plasma - Optical Emission Spectroscopy (ICP-OES).

REFERENCE

Černý, P and F.M. Simpson. 1978. The Tanco Pegmatite at Bernic Lake, Manitoba; X, Pollucite, *Canadian Mineralogist*. 16 (3): 325–333.

Table 1. Chemical composition of five pollucite samples.

Locality	SGS 1, Sinclair Caesium mine, WA, Australia	SGS 2, 1997 find, Himalaya mine, Mesa Grande, CA	SGS 3, Rose Quartz Crystal locality, Newry, ME	SGS 7, Valor southern pegmatite, Quebec, Canada	B12-226.2, Tanco mine, Manitoba, Canada
Oxide	**Wt.%**	**Wt.%**	**Wt.%**	**Wt.%**	**Wt.%**
SiO_2	43.80	43.70	43.50	45.80	46.09
Al_2O_3	15.30	15.40	15.40	15.70	16.38
Fe_2O_3	0.46	0.30	0.34	0.01	0.010
P_2O_5	0.31	0.04	0.24	0.02	0.00
CaO	--	--	--	--	0.01
Na_2O	1.77	1.62	1.77	2.17	1.74
K_2O	0.58	0.69	0.26	0.30	0.16
Rb_2O	0.469	0.30	0.444	0.39	0.74
MgO	0.03	0.06	0.01	0.02	0.003
Li_2O	0.127	0.17	0.198	0.196	0.43
Cs_2O	29.40	30.60	31.20	27.20	32.20
LOI	2.29	2.55	2.16	2.72	1.77
Totals	95.54	95.43	95.52	94.62	99.533
Si	1.987	2.113	2.101	2.003	2.112
Al	.818	0.877	0.877	0.809	0.885
Fe	.016	0.011	0.012	0.003	0.0003
Mg	0.002	0.004	0.001	0.001	0.000
P	0.02	0.002	0.010	0.001	0.0000
Na	0.156	0.152	0.166	0.184	0.155
Li	0.023	0.033	0.038	0.034	0.079
K	0.036	0.043	0.016	0.017	0.009
Rb	0.014	0.009	0.014	0.011	0.022
Cs	0.569	0.631	0.643	0.507	0.629
Si/Al	2.430	2.41	2.400	2.480	2.387
CRK	75.57	78.69	76.70	71.00	73.85

Analysis of pollucite samples including an example of a pollucite with the median refractive index (n=1.52) from Černý and Simpson (1978).

LOI = loss on ignition.

Atomic proportions were computed using 6 oxygen atoms. CRK is computed from CRK = 100 x [(Cs + Rb+ K)/(Cs + Rb + K + Na + Li)].

MINERALOGY OF THE FIELD PEGMATITE, AN EVOLVED REE-, BE-, AND TA-ENRICHED ANOROGENIC PEGMATITE FROM HART'S LOCATION, CARROLL CO., NEW HAMPSHIRE USA. *L. Lovering[1], A.U. Falster[2] and W.B. Simmons[2],* [1]96 Spring Rd., Milan, NH, 03588, [2]MP[2] Research Laboratory, Maine Mineral & Gem Museum, 99 Main St., Bethel, NH 04217.

The Field pegmatite is an intrusive dike exposed at an elevation of 670 m at Hart's Location in Carroll Co., NH. The dike cut through a small, 155 Ma (Eby 1994) A-type granitic pluton that was emplaced during a period of crustal extension. Initially intruded at a depth of approximately 1-2 km (Eby 1994), subsequent erosion and uplift have now exposed the dike at the surface. Miarolitic cavities of modest size are common in the dike.

The mineralogy consists of microcline in tan to white to pale green crystals and albite as white to colorless crystals up to 5 mm in maximum dimension, frequently seen as an epitaxial overgrowth on microcline. Quartz, typically dark smoky, is common as lustrous crystals over 5 cm in length. Biotite is found in the graphic parts of the pegmatite around pockets as lath-shaped crystals up to several cm in length. Muscovite occurs in some miarolitic cavities as well-formed crystals up to several cm across. Siderite with a minor rhodochrosite component is common and is typically replaced by hematite or goethite. The siderite crystals may reach several cm in maximum dimension and are either simple rhombohedra or more complex mosaic-textured rhombohedral crystals. Hematite occurs as mm-sized crystal plates on smoky quartz and other pocket minerals. Y-bearing fluorite ranges from colorless to pale purple to greenish and occurs in crystals with the following forms: {111} {100} and {110}) and as etched pieces up to several cm across. Rare astrophyllite in lath-shaped crystals up to several mm in length has also been found. Zircon rarely occurs as tiny crystals rarely exceeding 1 mm.

An unusual suite of Be, REE and Ta species occurs at this location: Bertrandite occurs in microcrystals as single crystals, twins, and trillings that sometimes include red helvite group species. Phenakite has been found in very complex short prismatic crystals up to 19 mm across. Helvite group species consists of danalite and a ruby-red crystal, which plots close to the midpoint of helvine, danalite, genthelvite (Fig. 1). REE species consist of fine, partially gemmy bastnäsite-(Ce) with elevated Nd and lower La content in crystals up to 2 mm maximum dimension. Fergusonite-(Y) and samarskite-(Y) occur in mm-sized brown crystals that are now metamict. Both monazite-(Ce) in brown crystals up to 4 mm across and allanite-(Ce) in mm-size crude dark brown masses also occur. Columbite group species have been found as platy to thick tabular crystals with elevated Mn and Ta contents. Surprisingly, widely spread microlite groups species also are found in mm-sized crystals of deep green, red, yellow and brown crystals. Chemically, the microlites are natro-calcio microlites with very pronounced Ta-dominance (Fig. 2). The late-stage Ta enrichment is similar to that found in the Nine Mile pluton in the Wausau complex (Falster et al. 2012).
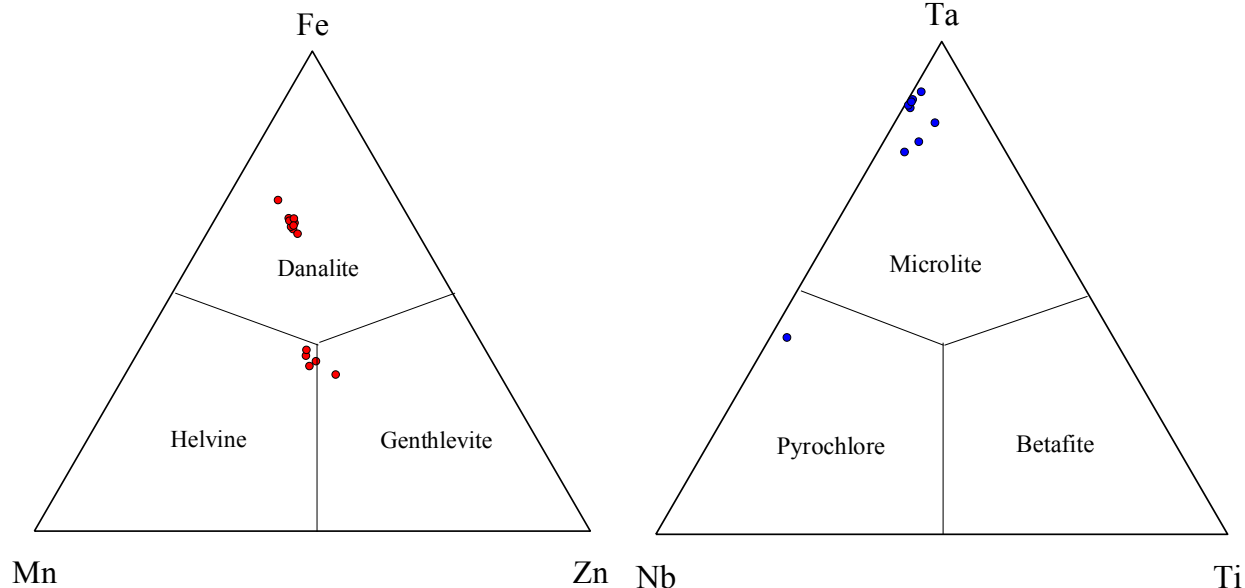
Fe / Mn / Zn ternary diagram with fields labeled Danalite, Helvine, Genthlevite.

Ta / Nb / Ti ternary diagram with fields labeled Microlite, Pyrochlore, Betafite.

Figure 1. Plot of the helvite group members from Hart's Location.

Figure 2. Ternary plot of the Y-site occupancy in microlite-pyrochlore species from Hart's Location.

REFERENCES

Eby, G.N. 1994. Third Hutton Symposium on Granites and Related Rocks. Part I: White Mountain Magma series. Third Hutton Symposium At: University of Maryland, College Park, MD. Volume: Pre-Conference Field Trip - Part I, 1-13.

Falster, A.U., T.W. Buchholz and Wm. B. Simmons. 2012. Mineralogical and mineral-chemical heterogeneity indicated by the distribution of accessory minerals in pegmatites of the Nine Mile pluton of the Wausau syenite complex, Marathon Co., Wisconsin. *Canadian Mineralogist* 50:1055-1070.

FLOWAGE IN THE ORE AT THE DWYER FLUORITE MINE, WILBERFORCE, ONTARIO: A MELT WAS INVOLVED! <u>R.F. Martin[1]</u> *and D. Schumann*[2], [1]Earth and Planetary Sciences, McGill University, 3450 University Street, Montreal, QC H3A 0E8, Canada, [2]Fibics Incorporated, 1431 Merivale Road, Ottawa, ON K2E 0B9, Canada.

The Dwyer mine, last worked for fluorite during the Second World War and now off limits, is located south of Cardiff Lake near Ironsides and Wilberforce, Ontario. It exploited dikes of white calcite with stringers of purple fluorite. Also carried in the slurry (Fig. 1) were green aegirine-augite, black amphibole, fragments of perthite (K-feldspar + albite), fluorapatite, titanite, quartz, britholite-(Y), bastnäsite-(Ce), thorite and zircon. Interestingly, the ribbons of fluorite drape around solid particles (Fig. 2). There is no doubt that flowage of particles occurred in the calcite matrix. To Frank D. Adams and Alfred E. Barlow, who mapped the area in 1910, the explanation would have been clear: in a metamorphic context, calcite flows plastically by gliding along cleavage planes. This had been amply shown experimentally by Adams; his pioneering work on

cylinders of calcite at 300° and 400°C and atmospheric pressure placed McGill University on the map as a center for deformation studies of minerals. But in the Grenville Province, temperatures and pressures were significantly higher, closer to 750°C and 7 kilobars ($\approx$ 25 km). Using an established workflow including large-area light microscopy image mosaics, Zeiss Atlas 5 large-area SEM imaging, and subsequent EDS and EPMA analyses, we present evidence that the flowing calcite matrix was a melt. Calcite embays fluorite, and contains islands of fluorite detached from the adjacent walls. In addition, the calcite carries euhedral to subhedral crystals of apatite against which fluorite had nucleated (shared a curvilinear boundary first with fluorite, then with calcite). It is clear that the calcite crystallized from a final melt of $CaCO_3$ composition, but micro-inclusions trapped in fluorapatite contain "jigsawed" calcite + fluorite, which shows that fluorapatite nucleated and grew in a melt containing carbonate, fluoride, phosphate and silicate. The complex melt crystallized in the sequence 1) fluorapatite, aegirine-augite and titanite, 2) fluorite, and 3) calcite.

Among the silicates carried in the slurry are grains of perthite. These consist of three feldspars, 1) orthoclase (dominant), 2) microcline, and 3) albite. They are texturally highly disturbed, such that the characteristic exsolution-induced texture is largely obliterated. Furthermore, they also contain patches of fluorite. These microxenolithic grains consist of fragments of the basement in the area. We believe that the perthite first homogenized and then melted briefly. Eventual cooling of the assemblage led to shrinkage due to thermal contraction and to incipient back-conversion of a neoformed disordered K-feldspar to microcline, which explains the presence of the fracture-filled rim of allanite-(Ce) that decorates the perthite grains.

The Dwyer mine occurs in an area mapped as an aureole of alkali-metasomatized (*i.e.*, fenitized) granite, now largely "syenitized". The metasomatism, which occurred 1070–1040 Ma ago, developed at the expense of granite emplaced in the interval 1230–1240 Ma. The metasomatism has enriched that granite in the alkalis, iron, the rare earths, titanium and fluorine. We believe that marble exposed close to the Dwyer mine melted, presumably at an advanced stage (*i.e.*, highest temperature) of the metasomatic event. The carbonate melt interacted with the metasomatic assemblages, and dissolved (*i.e.*, assimilated) them to become silicocarbonatitic. Fluorite is a powerful flux. It lowers the thermal stability of the melt phase in the binary system $CaCO_3$–CaF_2. It was efficiently dissolved in the carbonate melt. Our findings provide an explanation for the unusual calcite + fluorite dikes at the Dwyer mine, as well as in the nearby Schickler occurrence.

Figure 1. Flowage in the calcite dike, with ribbons of purple fluorite and entrained fragments of aegirine-augite, amphibole, apatite, perthite, and of the fenitized host-rock. Field of view: 30 cm. The photo, taken by Michael Adamowicz, is reproduced with permission.
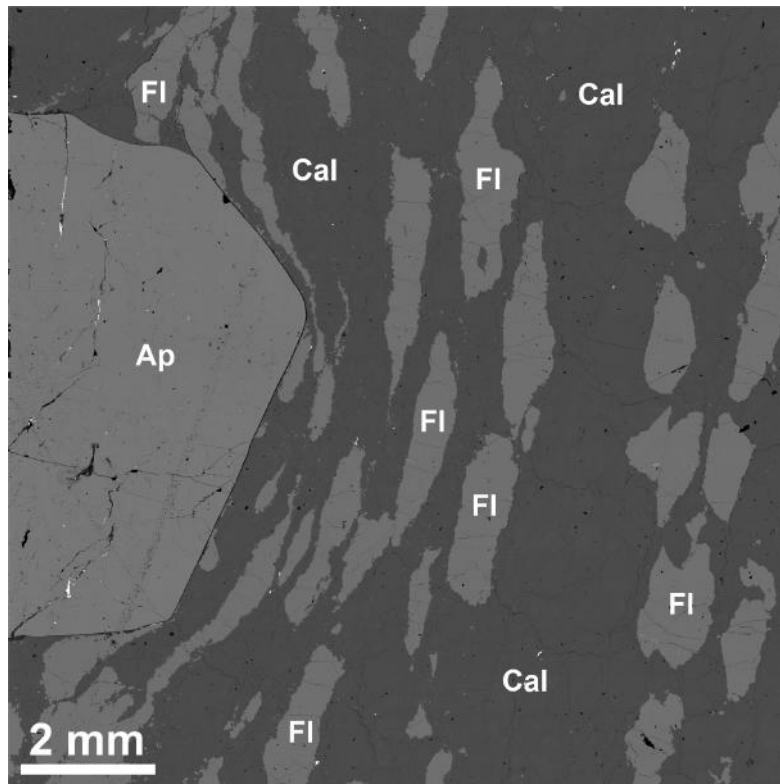

Figure 2. The ribbons of fluorite drape around the subhedral crystal of fluorapatite. Image extracted from the Zeiss Atlas 5 large-area image mosaic.

*MELT AND MICROMINERAL INCLUSIONS IN FLUORAPATITE, CALCITE, FLUORITE, ALBITE, AND AUGITE FROM THE SCHICKLER OCCURRENCE, ON, CANADA. <u>S. Mounce</u>, C. Emproto, M. Murchland, M. Rutherford, and J. Rakovan, Miami University Department of Geology and Environmental Earth Science, Oxford, Ohio, 45056.

The Schickler Occurrence is a public mineral collecting locality in Cardiff Township, Haliburton County, Ontario, Canada. In order to collect minerals on this property, permission must first be obtained from the Municipal office during regular business hours. For more information, please call (705) 448-2981. The workings at the Schickler Occurrence access a crustal carbonatite "vein dike" deposit where crystals of fluorapatite, albite, and augite to several centimeters are hosted within a dissociated calcite and fluorite matrix. This study of the Schickler Occurrence builds on a recent study by Schumann et al. (2019), which investigated melt inclusions within fluorapatite from the Yates Mine in Québec. Polished epoxy mounts of fluorapatite, calcite, fluorite, albite, and augite were prepared and analyzed using scanning electron microscopy and X-ray energy dispersive spectroscopy (SEM-XEDS) to identify and characterize inclusions. Micromineral inclusions were found to be ubiquitous, with each mineral having a unique inclusion assemblage. Multiphase inclusions interpreted to have crystallized from trapped melt, however, were almost exclusively found in samples of fluorapatite and more rarely in augite. These "melt" inclusions (Figure 1**)** are present as globules within the fluorapatite crystals. Phases present within these quenched melt inclusions identified using EDS include calcite, fluorite, rare earth element (REE) fluorcarbonate minerals, thorite, uraninite, and pyrite. In addition to melt inclusions, fluorapatite from the Schickler Occurrence hosts a profusion of inclusions of uraninite, thorite, thorianite, pyrite, yttrialite-(Y), calcite, allanite-(Ce), quartz, REE silicate phases, and at least three distinct REE fluorcarbonate minerals. It was also observed that green, hematite-free areas of fluorapatite crystals are markedly inclusion-free compared to red hematite-stained areas. Fluorite from the Schickler Occurrence hosts very few micromineral inclusions, whereas calcite, albite, and augite show a higher abundance, but markedly fewer inclusions than that hosted by fluorapatite. Finely disseminated inclusion phases identified within fluorite include yttriaite-(Y), synchysite, and REE phosphate phases, at 0.5-2 µm in size. Calcite hosts inclusions of yttriaite-(Y), REE fluorcarbonate minerals, and Cl-rich hydroxylbastnäsite. Albite crystals contain sparse inclusions of phlogopite, titanite, and domains of exsolved alkali feldspar. Augite is associated with anhedral jigsawed allanite-(Ce), a mineral rare in fluorapatite and absent in other inclusion assemblages. Augite contains inclusions of fluorite, allanite-(Ce), a pargasite group mineral, and quartz. The textures and mineralogy observed suggest that the carbonate-halide melt was heterogeneous and immiscible, resulting in separate fluorite and calcite melt inclusions. REE mineralization occurring in apparently altered zones of apatite, where hematite is abundant, suggests a late stage REE-bearing hydrothermal fluid, possibly sourced from the carbonate-halide magma during cooling.
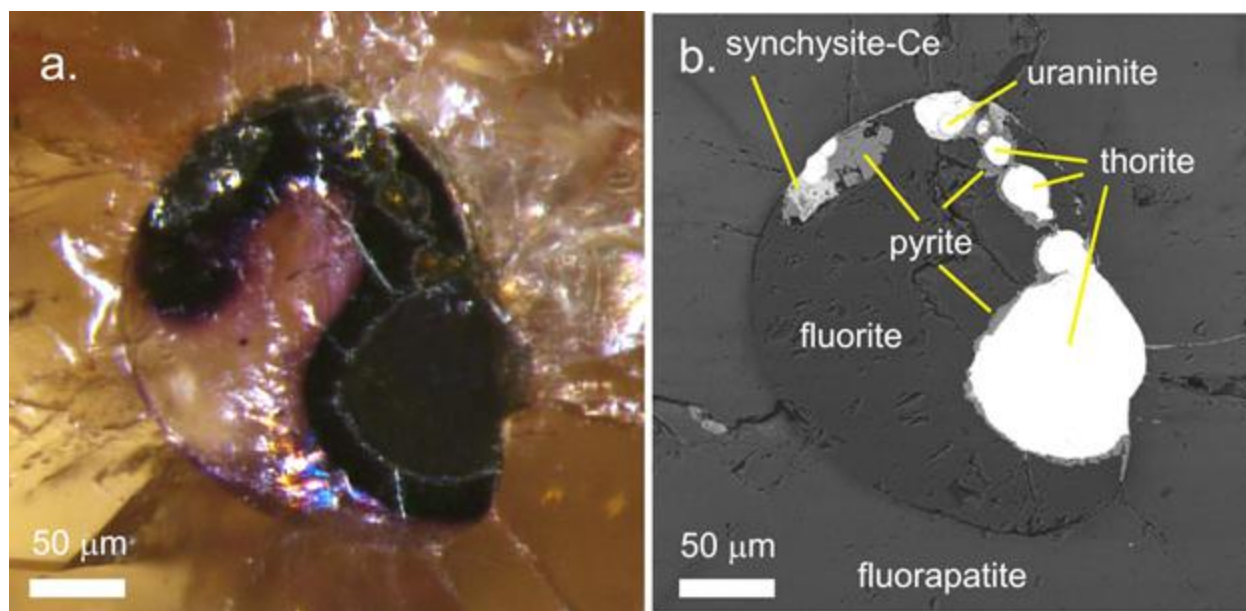
Figure 1. Polyphase melt inclusion within fluorapatite from the Schickler Occurrence imaged using light microscopy (a.) and backscattered electron imaging (b.). Darkening of the fluorite adjacent to radioactive minerals is observed in (a.). Brightness in (b.) is directly correlated with average atomic number (Z).

REFERENCES

Schumann, D., R.F. Martin, S. Fuchs, and J. de Fourestier. 2019. Silicocarbonatitic Melt Inclusions in Fluorapatite from the Yates Prospect, Otter Lake, Québec: Evidence of Marble Anatexis in the Central Metasedimentary Belt of the Grenville Province. *Canadian Mineralogist* 57:583–604. https://doi.org/10.3749/canmin.1900015.

*OPTICAL ANOMALIES IN FLATTENED INCLUSIONS FROM MUSCOVITE.
<u>M. Murchland</u>, M. Rutherford, J. Fink, and J. Rakovan, Department of Geology and Environmental Earth Science, Miami University, Oxford, OH, 45056.

The topic of flattened mineral inclusions within micas received a recent *exposé* in an article authored by John S. White in a 2018 issue of *Rocks & Minerals* magazine. The article reported on the appearance and characteristics of flattened crystal inclusions in muscovite, specifically almandine and gahnite from the Spruce Pine district of North Carolina and Delaware County Pennsylvania. White included the results of optical analyses performed by our research group on a flattened gahnite, which showed that the crystal exhibited a distinctly biaxial interference figure despite being an isometric mineral. In isometric crystals, the index of refraction is uniform in all directions and therefore should not exhibit any birefringence nor be capable of producing a coherent interference figure. Further research has indicated that the particularly strong interference figure (an acute bisectrix figure) observed in our analysis was the result of residual muscovite on the underside of the crystal.

However, after completely exposing a flattened gahnite crystal from another Spruce Pine sample, the same optically anomalous properties were observed, though the biaxial interference figure was much less intense and defined. Not only is the flattened gahnite birefringent, but it

also shows undulatory extinction and an acute bisectrix figure when viewed normal to the direction of flattening. By experimenting with the addition of mica of varying thickness to the optical path when viewing a flattened gahnite and garnet in crossed polars we found that the observed interference figure was the result of the mica even when exceedingly thin. We believe that this is the result of the very weak birefringence in the gahnite and garnet. Thus, light transmitted through the mica is only weakly disturbed when passing through the flattened inclusions.

Multiple flattened almandine crystals have also been extracted from muscovite books from Avondale, Pennsylvania. Like gahnite, garnet has an isometric crystal structure and therefore should exhibit isotropic properties when viewed in cross-polarized light. However, these crystals also exhibit birefringence. Double refraction in flattened almandine was noted as early as 1895 in crystals from North Carolina, however further details are lacking from this early work (Matthews 1895). When viewed in cross-polarized light, our flattened garnets exhibit undulatory extinction across the grain, suggesting that these are possible stress-induced optical anomalies.

Strain-induced birefringence has been recorded in multiple isometric minerals. Stress from plastic deformation, inclusions, impurities, fractures, and other defects can result in dislocations and lattice modifications that hold strain in the interior of the crystal. This alters the refractive indices in the strained zone and leads to anomalous optical characteristics. The studied gahnites and garnets most likely experienced initial stress from constrained growth within the muscovite sheets, leading to defects within the structure that hold the strain even after extraction from the muscovite. Strain from this occurrence is the likely cause of the optical anomalies observed in these typically isotropic minerals.
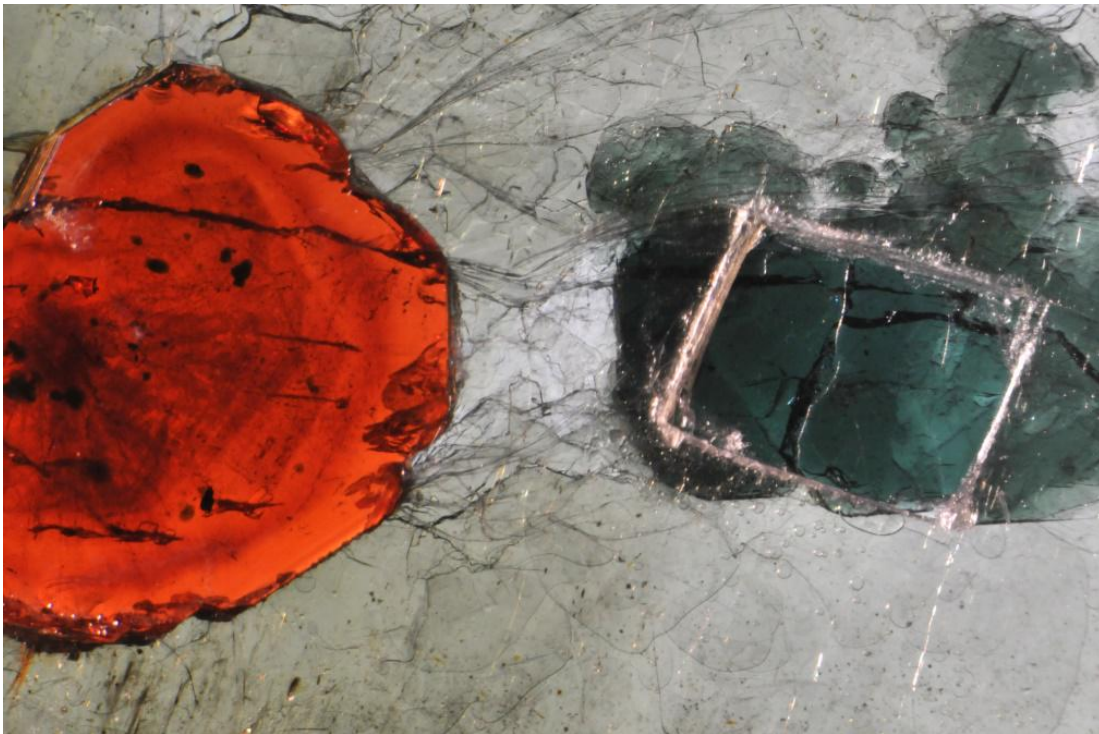

Figure 1. Flattened garnet (red, 7 mm across) and gahnite (green) inclusions in muscovite from the Deer Park Mine, Spruce Pine District, North Carolina. A window was cut through the muscovite to allow unencumbered optical measurements of the gahnite.
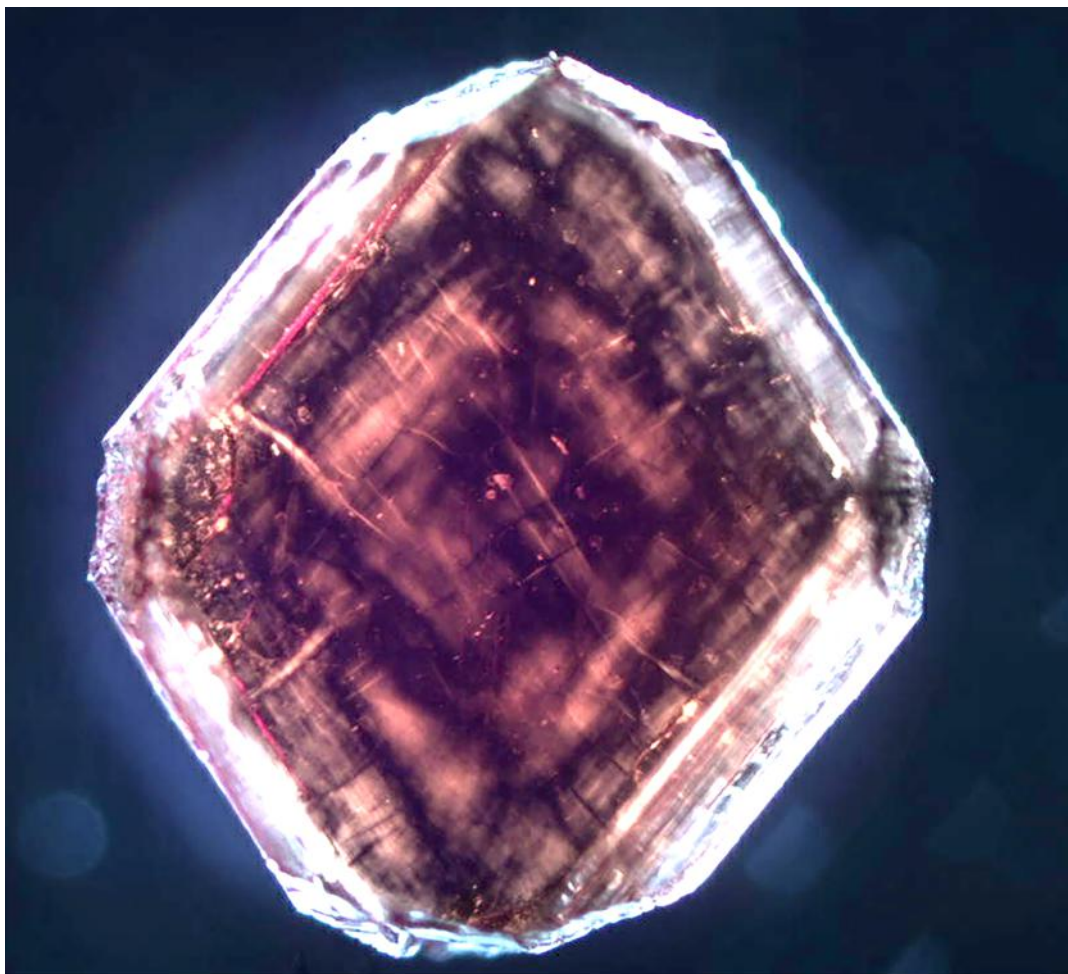
Figure 2. Flattened garnet from Avondale, PA (roughly 1 mm across) extracted from a muscovite sheet and placed under crossed polarizers, exhibiting anomalous extinction.

REFERENCES

Mathews, E. B. 1895. Notes on some flattened garnets from North Carolina. *Johns Hopkins University circular 121*.

White, J. S. 2018. Mineral Mysteries: Flattened crystals in muscovite. *Rocks & Minerals* 93:360-365.

*NEUTRON DIFFRACTION AND RESONANCE ABSORPTION SPECTROSCOPY STUDY OF THE HARVARD WIRE GOLD, GROUND HOG MINE, COLORADO. *J. Rakovan*[1]*, R. Alonso-Perez*[2]*, F. Keutsch*[3]*, S. Vogel*[4]*, A.S. Losko*[5]*, and A. Long*[6], [1]Dept. of Geology and Environmental Earth Science, 250 S. Patterson Ave., Miami University, Oxford, OH, 45056. [2]Mineralogical and Geological Museum, Harvard University, Cambridge, MA 02138, [3]Department of Chemistry and Chemical Biology, Harvard University, Cambridge, MA 02138, [4]Material Science & Technology Division, Los Alamos National Laboratory, Los Alamos, NM 87545, [5]The Heinz Maier-Leibnitz Center, Technical University of Munich,
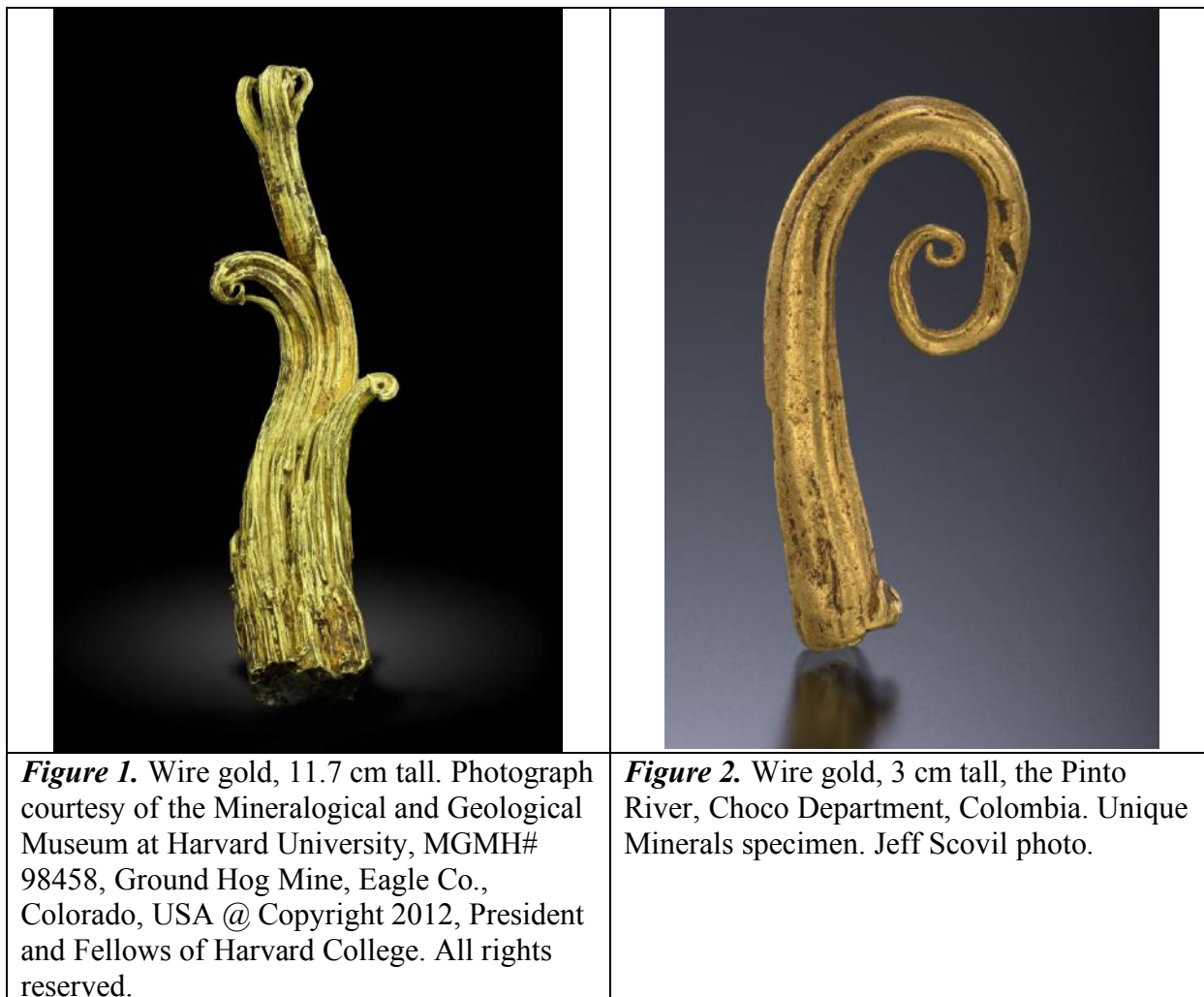
Garching Germany, [6]Material Science & Technology Division, Los Alamos National Laboratory, Los Alamos, NM 87545

Arguably the signature specimen of the Mineralogical and Geological Museum, Harvard University (MGMH) is the spectacular wire gold from the Ground Hog Mine in Red Cliff, Colorado. Many experts consider this to be the world's finest wire gold, and one of the premiere gold specimens because of the extreme rarity of the wire morphology, its size and the perfection of form. Sometimes referred to as the Ram's Horn, this iconic mineral specimen was donated to Harvard in 1947 with little information other than that it is gold. Originally labeled as from California, it was not until the late 1970's that its true provenance was rediscovered.

Recent studies have revealed a wealth of information about the crystallography, chemistry and growth mechanism of wire silver (Böllinghaus et al. 2018; Anderson et al. 2019) but almost nothing other than the existence of the morphology is known about wire gold. We have done the first detailed study of the crystallography and chemistry of wire gold. Three specimens, the Harvard Ram's Horn, a smaller wire gold from a placer deposit on the Pinto River, Colombia, and a wire silver from Yueshan deposit, China were taken to the Los Alamos Neutron Science Center (LANSCE) at Los Alamos National Laboratory (LANL) for analysis with neutrons. Because of the deeply penetrating nature of highly energetic neutrons the entire volume of such samples can be probed nondestructively.

Energy dispersive spectrometry (EDS) on a scanning electron microscope indicates that the surface of the Columbian wire is essentially pure gold while the Ram's Horn has roughly 30 wt.% silver alloying with the gold. Two neutron analytical techniques were used to probe the interior of the specimens. Neutron diffraction was conducted on the HIPPO (High-Pressure-Preferred Orientation) powder diffractometer. Energy resolved neutron imaging (ERNI) and Neutron resonance absorption spectroscopy (NRAS) were conducted on Flight Path 5. Because of concerns about neutron activation, only portions of the wire gold samples were analyzed. Diffraction data yield information about the crystallinity and texture of the interior of the samples. Data from the wire silver indicate a mosaic-like polycrystalline aggregate with many hundreds to thousands of crystals. Although subtle, there also appears to be a slight preferred orientation to the grains. This is consistent to the internal and external texture of wire silver analyzed by other methods (Böllinghaus et al., 2018; Anderson et al., 2019). Although the external morphology of the wire gold is very similar to that of wire silver, the internal texture is quite different. Both gold wires analyzed appear to be composed of only a few single crystals. Neutron spectroscopy data yield information about elemental and isotope chemistry. Similar to the EDS results NRAS shows that the interior of the Ram's Horn is alloyed with roughly 30 wt% silver. Interestingly, the bulk of the Columbian wire also contains silver at approximately 25 wt%. The contrast with EDS data (pure gold) is consistent with leaching of silver from gold-silver alloys when buried for long periods in placer deposits (Hough et al. 2007).

Differences between the internal texture of the wire gold samples and wire silver suggest that a different growth mechanism may be at play in the formation of wire gold. Alternatively, the presence of gold atoms may alter the same mechanism in ways that result in a different internal texture.

Figure 1. Wire gold, 11.7 cm tall. Photograph courtesy of the Mineralogical and Geological Museum at Harvard University, MGMH# 98458, Ground Hog Mine, Eagle Co., Colorado, USA @ Copyright 2012, President and Fellows of Harvard College. All rights reserved.

Figure 2. Wire gold, 3 cm tall, the Pinto River, Choco Department, Colombia. Unique Minerals specimen. Jeff Scovil photo.

REFERENCES

Anderson, C.A., R. Mathur, J. Rakovan and A. Tremsin. 2019. A New Metal Isotope Fractionation Effect by Solid-State Ion Conduction. *Geology*, 47:616-620.

Böllinghaus, T., V. Lüders, and G. Nolze. 2018. Microstructural insights into natural silver wires: *Scientific Reports*, 8:9053.

Hough, R. M., C. R. M. Butt, S. M. Reddy, and M. Verrall. 2007. Gold nuggets: Supergene or hypogene? *Australian Journal of Earth Sciences* 54:959–64.

UNUSUAL REE MINERALIZATIONS WITH FLUORBRITHOLITE, TÖRNEBOHMITE, AND CERITE NEAR JAMESTOWN, COLORADO, USA: PETROCHEMISTRY, ORIGIN, AND ROLE OF LIQUID IMMISCIBILITY. _M.B. Raschke[1], C. Stern[2], J. Ross[2], J. Allaz[3], L. Farmer[2], A. Skewes[2], and P.M. Persson[4]_, [1]Department of Physics, Department of Chemistry, and JILA, University of Colorado, Boulder, CO 80309-0390 USA, [2]Department of Geological Sciences, University of Colorado, Boulder, CO 80309-0399 USA, [3]ETH Zurich Institute für Geochemie und Petrologie, 8092 Zurich, Switzerland, [4]11655 West 28th Place, Lakewood, Colorado 80215 USA.

Two unusual rare earth element (REE) mineralization localities occur within the anorogenic 1.4 Ga Longs Peak-St. Vrain Silver Plume-type intrusion near Jamestown, Colorado (USA). Although discovered early (Goddard and Glass 1940), and recognized for their globally unique mineral assemblage and association, they have for long received only limited attention. We present results from an ongoing systematic investigation into the REE mineralization and its origin (Allaz et al. 2015, Stern et al. 2018).

Irregular-shaped centimeter- to decimeter-sized mineralized pods and veins (Fig. 1, left) consist of zoned mineral assemblages dominated by fluorbritholite-(Ce) in a gray-colored core up to 10 cm thick, with monazite-(Ce), fluorite, and minor quartz, uraninite, and sulfides. The core zone is surrounded by a black, typically millimeter-thick allanite-(Ce) rim, with minor monazite-(Ce) in the inner part of that rim. Bastnäsite-(Ce), törnebohmite-(Ce), and cerite-(Ce) appear in a thin intermediate zone between core and rim, often just a few hundreds of micrometers wide (Fig. 1, right). Electron microprobe analyses show that the overall REE content increases from core to rim with a disproportionate increase of heavy REE compared to light REE. Cerite-(Ce) is only a minor constituent of the thin zone between the inner rim and the core. A combination of textural features and geochemical data suggest that the aplite and REE-rich globular segregations co-existed as two co-genetic liquids prior to their crystallization, and we propose that they are formed by silicate–fluoride+phosphate ($+S+CO_2$) melt immiscibility following ascent, cooling, and decompression of what was initially a single homogeneous magma that intruded the granite. Although monazite-(Ce) and uraninite U–Th–Pb microprobe ages for the segregations yield 1.420($\pm$25) and 1.442($\pm$8) Ga, respectively, thus suggesting a co-genetic relationship with their host granite, average $\varepsilon_{Nd1.42Ga}$ value of -3.9 for the granites and related granitic pegmatites differ from the average value of -1.6 for both the aplites and REE-rich segregations. These data are consistent with the aplite dikes and the REE-rich segregations they contain being co-genetic, but derived from a source different from that of the granite.
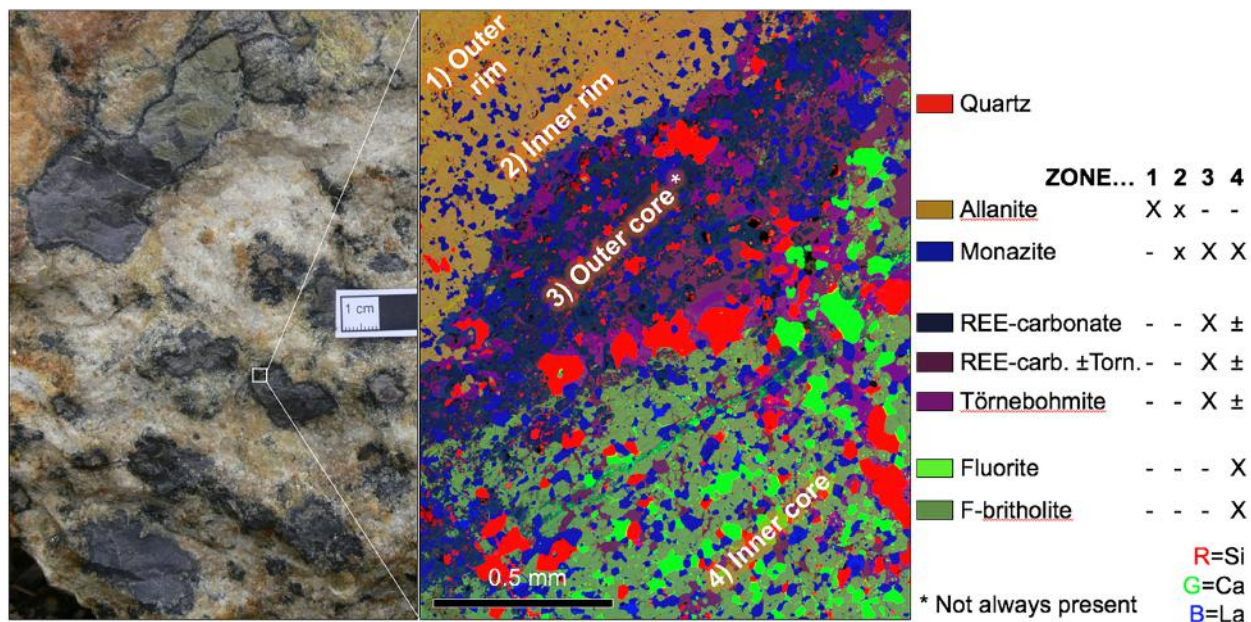

Figure 1. Image of REE-rich globules within aplite dikes (left) characterized by allanite rims surrounding purple/grey fluorbritholite-(Ce)+fluorite+monazite-(Ce) cores. Composite color X-ray map showing the type and spatial relationship of the REE mineralization at the rim to core transition (right, X = major phase, ± = minor phase).

REFERENCES

Allaz, J., M.B. Raschke, P.M. Persson, C.R. Stern. 2015. Age, petrochemistry, and origin of a REE-rich mineralization in the Longs Peak-St. Vrain batholith near Jamestown, Colorado (USA). *American Mineralogist* 100:2123-2140.

Goddard, E.N. and J.J. Glass. 1940. Deposits of radioactive cerite near Jamestown, Colorado. *American Mineralogist* 25:381-404.

Stern, C.R., J.M. Allaz, M.B. Raschke, G.L. Farmer, M.A. Skewes, and J.T. Ross. 2018. Formation by silicate-fluoride+phosphase melt immiscibility of REE-rich globular segregations within aplite dikes. *Contributions to Mineralogy and Petrology* 173:65.

*OPTICALLY ANOMALOUS CRYSTALS. <u>M. Rutherford</u>, M. Murchland, J. Fink, and J. Rakovan, Department of Geology and Environmental Earth Science, Miami University, Oxford, Ohio 45056, U.S.A.

One of the most powerful techniques for the study of minerals is transmitted light optical microscopy of thin slices between polarizers whose polarization directions are oriented ninety degrees to one another. This configuration is known as crossed polars. The optical behaviors of crystals explored in this way are constrained by the symmetry exhibited by their atomic arrangements. Each crystal system (i.e. isometric, monoclinic, etc.) exhibits specific optical characteristics, which can be used in mineral identification as well as structural and chemical characterization. However, the optical characteristics exhibited in some crystals do not conform to the crystal systems that they are thought to belong to. Few (if any) natural crystals are internally perfect, having no defects. Such imperfections may give rise to 'optically anomalous' crystals with peculiar optical behavior. Optical anomalies may be caused by several different mechanisms, but always involve a change in symmetry, usually a reduction. Optically anomalous behavior may result from physical stress on a crystal. When physical stresses are exerted on a crystal, strain is experienced by the internal structure as defects migrate, and the bond geometry is distorted. Strain and the migration of defects occur during plastic flow associated with regional metamorphism, the results of which are easily visible in minerals such as quartz, that exhibit undulatory extinction. Internal stress resulting from, for example chemical heterogeneities or radiation damage, can also strain a crystal structure and cause optically anomalous behavior.

Another important cause of optically anomalous behavior is reduction in symmetry due to ordering of different elements among crystallographic sites within a crystal. Such ordering can take place after a crystal has grown, by diffusion, or during the growth process by differential incorporation at structurally distinct surface sites. An example of post growth ordering is microcline that has formed from the ordering of Si and Al among the tetrahedral sites in the structure of precursor sanidine or orthoclase. The lowering of symmetry associated with this ordering transition leads to the common "tartan twinning" observed in plutonic igneous rocks.

Ordering of atoms can also occur during growth. This is commonly seen in sectoral and intrasectoral zoning of optical anomalies. A region of a crystal that has formed by incorporation of atoms onto a specific crystal face constitutes a sector. Sectoral zoning is a difference in chemistry or a physical property such as optical character among sectors (Rakovan 2009). This usually involves sectors of symmetrically nonequivalent faces; however, in the case of ordering it can involve equivalent sectors. This phenomenon is well-known from minerals such as apatite.

A petrographic thin section of an apatite cut perpendicular to [001] would be expected to remain extinct when viewed in crossed polars, as this is the orientation of the optic axis when apatite is hexagonal. However, apatite crystals from Ohio (Richards and Rakovan 2000) instead display birefringence with sectorally varying extinction angle (i.e. optical orientation). In a related phenomenon, intrasectoral zoning (Reeder and Rakovan 1999), regions of distinct optical orientation are constrained to subsectors under growth hillocks on crystal faces. Figures 1 and 2 show this phenomenon in garnet and apatite.

Transmitted light microscopy between crossed polars is extraordinarily sensitive to subtle reductions in symmetry and thus may reveal interesting mineralogical characteristics unobservable by other methods of analysis. For this reason, it is important to continue studying optical anomalies and what they tell us about crystals.
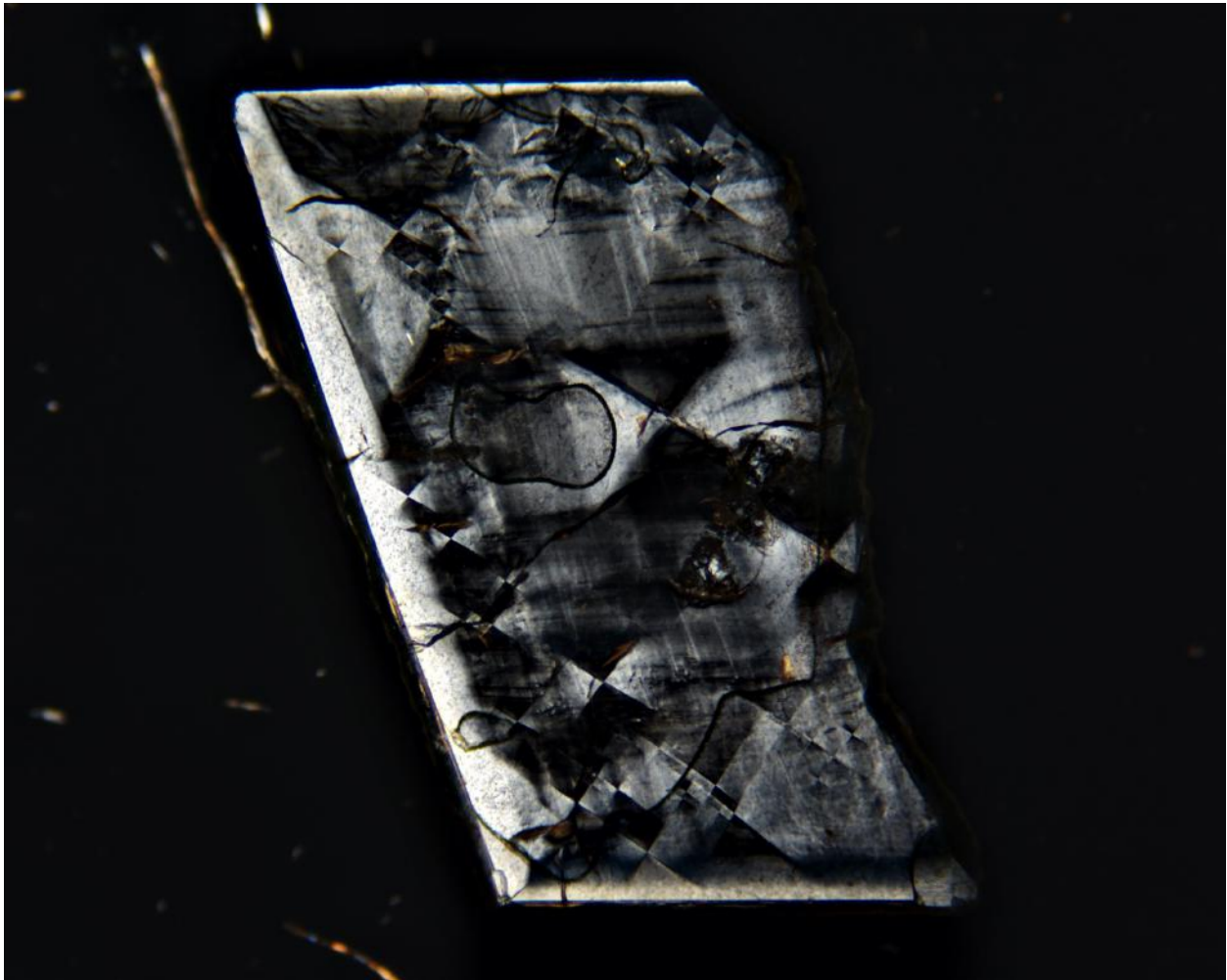

Figure 1. Photomicrograph of a (110) section of grossular garnet, from the Jeffrey Mine, Canada, in crossed polars showing intrasectorally distributed anomalous birefringence sometimes referred to as sector twinning.
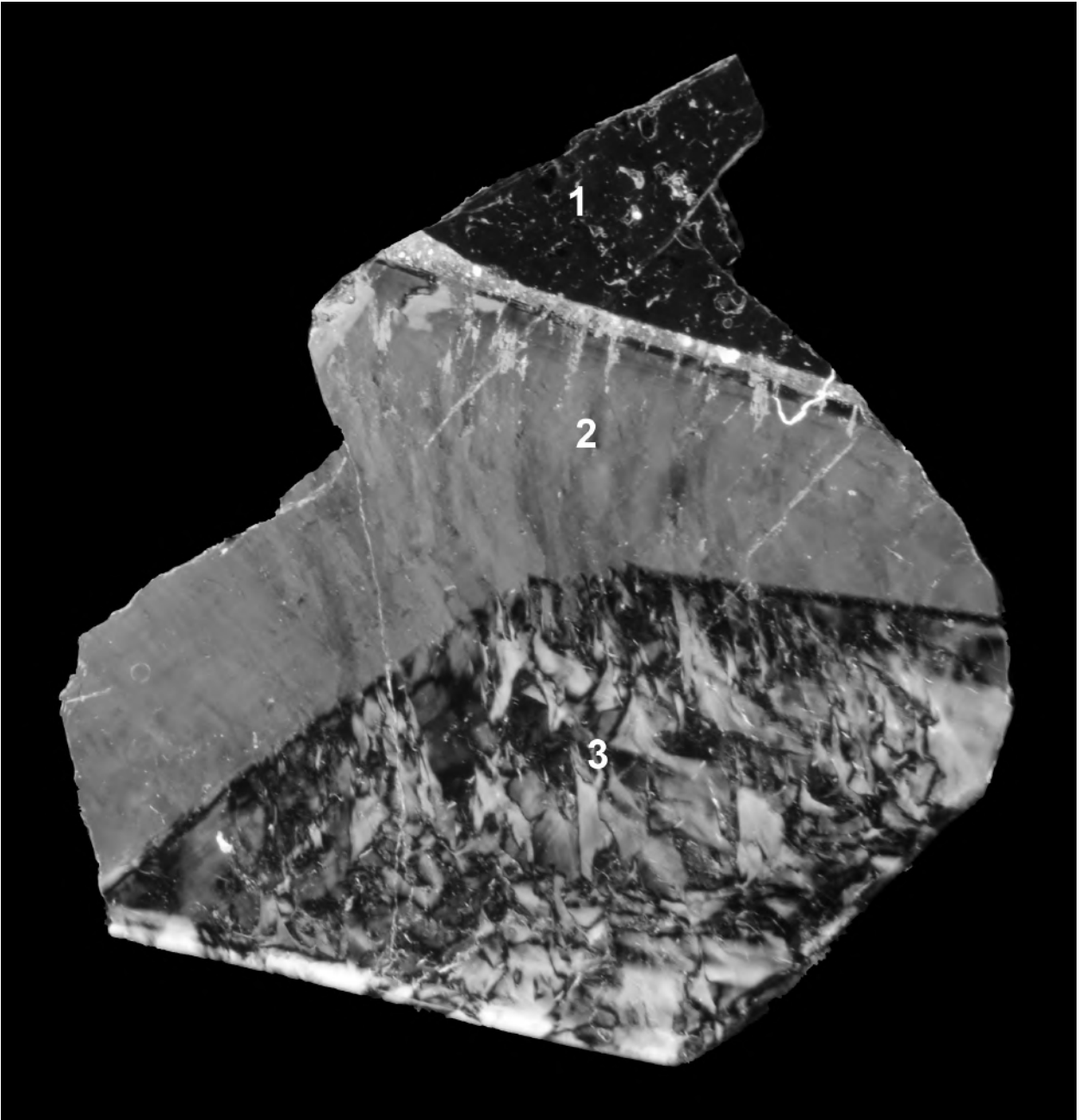
Figure 2. Photomicrograph of a 1-cm zoned hydroxylapatite/fluorapatite crystal (001) section taken in crossed polars. Optically distinct zones are (1) normal uniaxial character (2) strain related birefringence, and (3) intersectoral zoning. From Richards, Kelly and Rakovan 2018.

REFERENCES

Rakovan, J. 2009. Word to the Wise: Sectoral Zoning. *Rocks & Minerals* 84:171-176.

Reeder, R.J. and Rakovan, J. 1999. Surface structural controls on trace element incorporation during crystal growth. In Growth, Dissolution and Pattern-formation in Geosystems, B. Jamtveitand P. Meakin (eds.) p. 143-162. Kluwer Academic Publishers.

Richards, R.P. and J. Rakovan, J. 2000. 27th Rochester Mineralogical Symposium, Contributed Papers in Specimen Mineralogy: The first occurrence of apatite crystals in Ohio. Rochester Mineralogical Symposium. *Rocks and Minerals* 75: 255.

Richards, H., S. Kelly, and J. Rakovan. 2018. 44th Rochester Mineralogical Symposium, Contributed Papers in Specimen Mineralogy: Structural and chemical complexities of hydroxylapatite from the Sapo Mine. Brazil. *Rocks & Minerals* 93:460-461.